Computational Materials Science 47 (2010) 857–866

Contents lists available at ScienceDirect

Computational Materials Science

journal homepage: www.elsevier.com/locate/commatsci

Coupled thermo-mechanical FE simulation of the hot splitting spinning process of magnesium alloy AZ31

He Yang *, Liang Huang, Mei Zhan

State Key Laboratory of Solidification Processing, School of Materials Science and Engineering, Northwestern Polytechnical University, P.O. Box 542, Xi'an 710072, China

ARTICLE INFO

Article history:
Received 13 August 2009
Received in revised form 4 October 2009
Accepted 10 November 2009
Available online 1 December 2009

PACS:
02.60.Cb
81.20.Hy
81.40.Gh
62.20.fk
81.40.Lm

Keywords:
Coupled thermo-mechanical
FE simulation
Hot splitting spinning
Magnesium alloy AZ31
Field distributions
Forming quality

ABSTRACT

Magnesium alloy AZ31 shows excellent ductility and formability at elevated temperatures, and using hot splitting spinning it can be formed into a structural component subjected to impact loadings, such as, a wheel hub of aero undercarriage or kinds of light whole wheels. In this paper, based on the analysis of microstructures and deformation characteristics of magnesium alloy AZ31, a reasonable deformation temperature range is obtained during the thermoplastic forming process. Adopting a flow stress model of magnesium alloy AZ31 considering the dynamic recrystallization (DRX), a 3D elastic–plastic FE model of hot splitting spinning of magnesium alloy AZ31 is established based on the FEM software platform of ABAQUS/Explicit and a developed 3D-FE model of cold splitting spinning, and its reliability is validated. Furthermore, field distributions of deformed component, including temperature fields, stress fields and strain fields, and variations of different nodal temperatures are obtained. And the influencing laws of different initial temperatures of disk blank and different feed rates of splitting roller on forming quality of deformed flanges are investigated, consequently the optimal forming temperature is approximate 300 °C and the optimal feed rate of splitting roller ranges from 1 to 3 mm/s during the hot splitting spinning process of magnesium alloy AZ31. The results may help to understand the forming characteristics and optimum design of the hot splitting spinning process.

1. Introduction

As one kind of lightweight alloys in the widely applications, magnesium alloys are currently the lightest structural materials with low density, high specific strength and specific stiffness, superior damping capacity [1–3]. The superior damping capacity is provided by the lower Young's modulus-*E*, and the value of *E* is no sensitive to material microstructures. When a structural component of magnesium alloy is subject to the same impact loadings, it can perform more elastic deformation and absorb more impact energy. Besides, stress distributions inside of a structural component of magnesium alloy are more uniform, thereby high stress concentrations can be avoided. Therefore, a structural component of magnesium alloy subjected to the impact loadings can be formed. Meanwhile, as one new continuous and local plastic forming technology, splitting spinning is designed to split a revolving disk blank from the outer rectangular edge into two flanges using a roller called splitting roller with a sharp corner, and then shaping spinning is done by two or three other forming rollers [4,5], as shown in Fig. 1. Compared with other conventional methods combining with casting, forging and welding and then mechanical processing, splitting spinning has the remarkable advantages of high efficiency, low cost and good flexibility, and its products for aeronautics, astronautics, automobile and weapon industry meet the high quality and high precision demands and are developed at low costs in short time [6–9]. Accordingly, based on the above remarkable advantages and application foregrounds of magnesium alloy AZ31 and the above manufacturing predominance of splitting spinning, a structure component of magnesium alloy AZ31 subjected to the impact loadings and with high quality and high precision can be formed using hot splitting spinning, such as, a wheel hub of aero undercarriage or kinds of light whole wheels.

According to the past research on deformation property of magnesium alloy, the ductility and formability of magnesium alloy is low at room temperature due to its hexagonal close-packed (hcp) crystal structure, so it is difficult to be deformed. However, it shows excellent ductility and formability at elevated temperatures [10]. Especially, magnesium alloy AZ31 is characterized by a good formability and ductility at elevated temperature [11]. The investigation by Ogawa et al. [12] indicated that the determination of appropriate forming temperature of magnesium alloy AZ31 is

* Corresponding author. Tel./fax: +86 29 8849 5632.
E-mail address: yanghe@nwpu.edu.cn (H. Yang).

0927-0256/$ - see front matter © 2009 Elsevier B.V. All rights reserved.
doi:10.1016/j.commatsci.2009.11.014

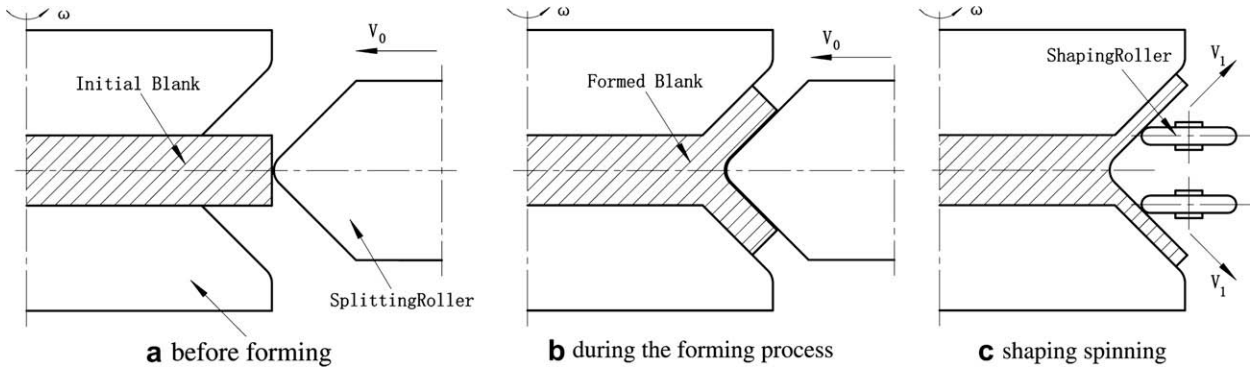

Fig. 1. Schematic illustration of the splitting spinning process.

one of key factors, thereby the forming limit is improved and the fracture of specimen is avoided. The investigation by Doege and Droder [13] indicated that high forming limit of magnesium alloy AZ31 could be obtained when the forming temperature exceeds 200 °C, on the contrary, forming limit reduced and forming quality of a structural component decreased when forming temperature reaches above 450 °C. Consequently, many recent research activities show that, magnesium alloy AZ31 has the features of the high plastic formability from 200 °C to 450 °C [14], and it can be deformed into desired a structural component.

Due the limitation of experimental study and theoretical analysis, the investigations on the distributions of stress, strain and temperature and the influencing laws of forming parameters on forming quality are difficulties during metal deformation processes. FE numerical simulation is applied increasingly and is becoming a very important tool for the research on the field distributions and forming quality of a structural component [15–18]. At present, there exists only some research on the FE numerical simulations of splitting spinning. Based on the FE software DEFORM2D V5.02 and MARC/Autoforge V1.2, Hauk et al. [19] studied the forming characteristics and rules of splitting spinning using elastic–plastic FEM, and the mechanism and laws of geometric dimensions of disk blank and friction influencing on deformation during the process are obtained under the two-dimensional space. And then experimental research are performed by means of the equipments called Tooling System, the influencing laws of different materials, different feed rates and different splitting spinning angles on splitting spinning force during the process are obtained [20]. The deviation between two-dimensional simulation data and experiment data is acceptable, so the results are usable. Nevertheless, the 3D-FE model reduced disk blank, simplified feeding mechanism system and ignored friction action between disk blank and supporting roller during the process in order to reduce computational time and improve computational efficiency. So, the above assumptions resulted in lower computational precision, such as, the splitting spinning force in simulations was less than the one in experiments, about one half. So in order to obtain more accurate simulation results, a reliable and practical 3D-FE model of splitting spinning should be established.

The authors have studied the cold splitting spinning process of aluminium alloy [21–24]. A reliable and practical 3D-FE model of cold splitting spinning of aluminium alloy is established, and the variations of spinning force, stress fields and strain fields with time are obtained [21]. The influencing laws of forming parameters of splitting spinning on the quality and precision of flanges are investigated based on the forming characteristics of splitting spinning combining with the behaviors of roller [22]. The influencing laws of material parameters on splitting spinning force, splitting spinning moment and forming quality of flange have been investigated [23]. A reliable theoretical model established by the principal stress method is proposed for the calculation of splitting spinning force, and the influencing laws of forming parameters on splitting spinning force are investigated [24]. However, the research on hot splitting spinning of magnesium alloy AZ31 is scant by now, so the above results may help study hot splitting spinning of magnesium alloy AZ31.

In this paper, according to the analysis of microstructures and deformation characteristics of magnesium alloy AZ31, the reasonable forming temperature range is obtained during the thermoplastic forming process. Adopting a flow stress model of magnesium alloy AZ31 considering the dynamic recrystallization (DRX), a 3D elastic–plastic FE model of hot splitting spinning for magnesium alloy AZ31 is established based on the FEM software platform of ABAQUS/Explicit, and then the reliability is verified by theoretical evaluation. Furthermore, field distributions of deformed component, including temperature fields, stress fields and strain fields, and variations of different nodal temperature are obtained. And the influencing laws of different initial temperatures of disk blank and different feed rates of splitting roller on the forming quality and precision of deformed flanges are investigated, consequently the optimal forming temperature and the optimal feed rate of splitting roller during the hot splitting spinning process of magnesium alloy AZ31 are obtained.

2. Research methodology

2.1. Microstructures and deformation characteristics of magnesium alloy AZ31

The deformation mechanisms of magnesium alloy mainly contain twinning and slip, and deformation texture roots in basal slips among grain boundaries [25–27]. All these deformation mechanisms and texture characteristics affect plastic deformation behaviors, formability and mechanical property of magnesium alloy strongly. During the hot splitting spinning process, magnesium alloy AZ31 (Mg–3mass%Al–1%massZn–0.5%massMn) disk blank is mainly extruded, so microstructures of the extrusion specimen in different forming temperatures must be realized in order to obtain the optimal forming parameters and forming temperature range.

Thermal mechanical property of magnesium alloy AZ31 is quite related to processing technology, heat treatment process and so on, especially when different forming temperatures, thermal mechanical property of magnesium alloy AZ31 varies on a large scope. Therefore, according to the analysis of microstructures and deformation characteristics of magnesium alloy AZ31, thermoplastic deformation mechanism are obtained. And then the forming rules during the hot splitting spinning process of magnesium alloy AZ31 under tensile stress and compressive stress simultaneously is

revealed and the optimal forming parameters and forming temperature range are obtained.

According to excellent ductility and formability at elevated temperatures and high temperature variation from 200 °C to 450 °C, there are two kinds of specimen [27], which are the extrusion magnesium alloy AZ31 processed by extruding at 500 °C is called the sample A (exceeding the high temperature variation) and the extrusion magnesium alloy AZ31 processed by extruding at 210 °C is called the sample B (within high temperature variation). Fig. 2 is shown as microstructure of magnesium alloy AZ31 specimen, (a) sample A and (b) sample B [27]. Usually, the plasticity or ductility of magnesium alloy AZ31 is low at room temperature, but at elevated temperatures, plastic deformation energy is activated among grains and grain boundaries, so the plasticity and forming limit are improved.

For magnesium alloy AZ31, forming temperature must be controlled from 200 °C to 450 °C. Because plastic deformation energy is inactivated among grains and grain boundaries below 200 °C, and disk blank of magnesium alloy AZ31 may brittle fracture easily, nevertheless, when temperature being above 450 °C, disk blank of magnesium alloy AZ31 may be oxide etch and grain size may become large, even phase transformation arises and plasticity decreases, as shown in Fig. 2a. According to Fig. 2, it can be found that, microstructure of sample A shows large grain size obviously and the average grain size is 71 μm for sample A, and microstructure of sample B shows close and small grain size and the average grain size is 8 μm for sample B.

According to the analysis of microstructures, the energy of twin interfaces is significantly large for magnesium alloy AZ31 and twin nucleation decreases with decreasing grain size. The plasticity and formability of magnesium alloy AZ31 is low and the response of plastic deformation is inadequacy below 200 °C. But when magnesium alloy AZ31 at elevated temperatures, the plastic deformation energy transforms internal energy and the forming process is done successfully and well, consequently the requirement of close and small grain size in a whole structural component is satisfied. Meanwhile, it is necessary to control the upper limit of forming temperature in order to avoid oxide etch and large grain size in the whole structural component of magnesium alloy AZ31, even phase transformation.

Furthermore, due to dynamic recovery (DRV) and dynamic recrystallization (DRX), deformation magnesium alloy shows distinct high temperature softening during the hot splitting spinning process. The strain softening is the typical characteristic of the elevated flow stress model of magnesium alloys, whose material response can principally be divided into two categories during the hot forming process, DRV type and DRX type. For magnesium alloy AZ31, DRX is the main characteristic of flow stress curves [28]. And also, the temperature of dynamic recrystallization (DRX) of magnesium alloy AZ31 is approximate from 533 K to 593 K [28].

According to above microstructures and deformation characteristics of magnesium alloy AZ31 with the characteristics of homogeneous and isotropic elastic–plastic body, it is necessary to satisfy the condition of five independent slips at the beginning of plastic deformation, afterward the relaxation mechanisms for the stress concentration of plastic deformation at the grain boundaries are important at a subsequent or final forming stage. Besides, the plastic deformation mechanisms depend on the grain size. Furthermore, magnesium alloy AZ31 shows excellent ductility and plasticity when forming temperature ranges from 200 °C to 450 °C. Therefore, plastic deformation mechanisms of magnesium alloy AZ31 and research foundations of hot splitting spinning of magnesium alloy AZ31 are obtained.

2.2. Coupled thermo-mechanical FE model of hot splitting spinning of magnesium alloy AZ31

2.2.1. Constitutive equation for magnesium alloy AZ31

Microstructures during the thermal plastic forming process reflects constitutive equations of thermal plastic deformation on the macroscopic view, namely, the flow stress model with the characteristics of temperatures, strain rate, strain and microstructure evolution. It represents one basic variable during the hot forming process, and determines the loadings quantity and the required energy magnitude.

The flow stress curves of magnesium alloy AZ31 at various strain rate is shown in Fig. 3 [28]. According to Fig. 3, the characteristics of magnesium alloy AZ31 stress–strain curves are represented as follows: (1) In the initial stage of the forming process, the stress abruptly increases to a peak due to the dominance of work hardening. (2) When the strain rate increases while the temperature is fixed, or the temperature decreases while the strain rate keeps unchanged, the overall level of the flow stress curve enhances correspondingly due to the growing work hardening. (3) When deformation exceeds the peak strain, the flow stress decreases at a rate which reduces with increasing strain as softening caused by DRX overtakes hardening caused by work hardening. (4) The flow stress shows steady-state region due to the equilibrium of work softening and work hardening finally. Consequently, a reasonable constitutive equations of magnesium alloy AZ31 which satisfies above deformation characteristics in the study is adopted as follows [28]:

$$\ln \sigma = \psi(\varepsilon - \varepsilon_p)^2 \ln \xi\varepsilon + \ln \sigma_p, \tag{1}$$

where σ is plastic stress, ε is plastic strain, σ_p is the peak stress, ε_p is the peak strain, the value of parameter ξ is 0.6993, and the value of parameter ψ is 1.683 at the following deformation conditions: the temperature – T less than or equal 523 K, T less than or equal 573 K and strain rate – $\dot{\varepsilon}$ greater than or equal 0.1 s^{-1}, T less than

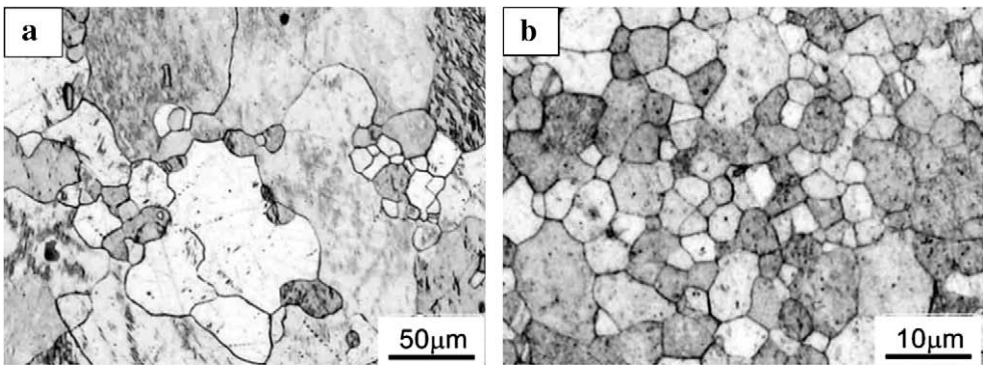

Fig. 2. Microstructure of magnesium alloy AZ31 extrusions, (a) sample A and (b) sample B [27].

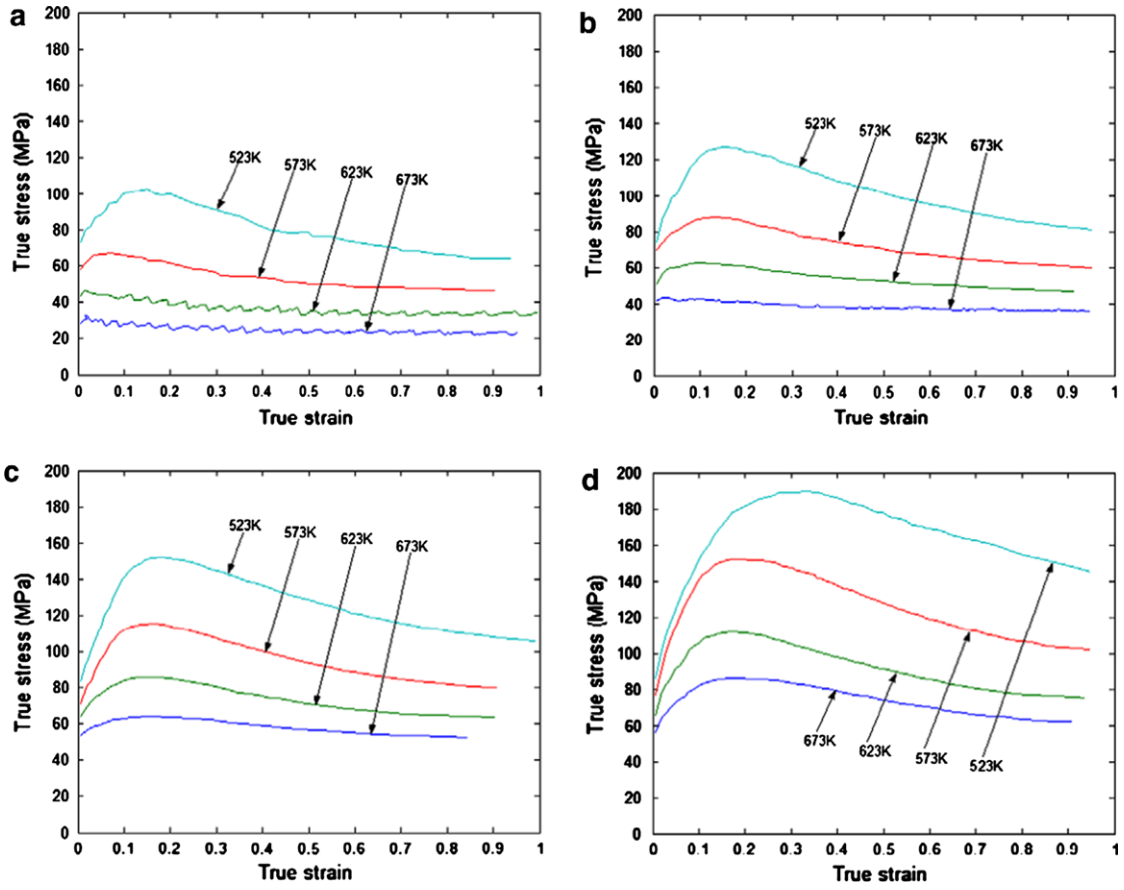

Fig. 3. Schematic of the stress–strain curves of magnesium alloy AZ31 at various strain rate: (a) $\dot{\varepsilon} = 0.001^{-1}$, (b) $\dot{\varepsilon} = 0.01^{-1}$, (c) $\dot{\varepsilon} = 0.1^{-1}$, and (d) $\dot{\varepsilon} = 1^{-1}$ [28].

or equal 623 K and $\dot{\varepsilon}$ greater than or equal 1 s^{-1}; and the value of ψ equals to 1.28 at the other deformation conditions. The stress–strain curves of magnesium alloy AZ31 considering both macroscopic behavior and microscopic mechanism express the sensitivity of flow stress to temperature, strain rate, strain and microstructure evolution. This model of flow stress is in good agreement with the experiments data and has higher precision. The standard deviation between the model prediction values and the experiments data is approximately 2.32%. So, as far as the elevated deformation is concerned, this model can be applied to hot splitting spinning of magnesium alloy AZ31.

2.2.2. Establishment and verification of FE model

The heat transfer during the hot splitting spinning process is a very complicated coupled thermo-mechanical problem. During the process, the free surface of disk blank exchanges heat with external environment in manner of convection and radiation, and the contact surface conducts heat to the dies. Meanwhile, the plasticity deformation energy of disk blank is mostly converted into heat energy and internal energy. The interaction of the above-mentioned two factors makes it difficult to analyze the thermal–mechanical problem of hot splitting spinning accurately with analytical method, while the numerical method, especially finite element method, is feasible and effective. In FE modeling process, material is a homogeneous and isotropic elastic–plastic body, and follows von Mises yield criterion and shear friction model [29].

Consequently in this study, according to the past research [21], based on the FEM software platform of ABAQUS/Explicit, a 3D elastic–plastic FE model of hot splitting spinning of magnesium alloy AZ31 is established, as shown in Fig. 4. Diskblank is defined as a 3D deformable solid body, SplittingRoller is defined as an analytical rigid body, and two Mandrels are defined as discrete rigid bodies. The FE model is reliable and reasonable by the validation of the past research [21]. Due to joining the thermal analysis procedure, it is necessary for hot splitting spinning of magnesium alloy AZ31 to carry out the theoretical evaluation [30,31]. In order to indicate the FE results being a receivable quasi-static solution, there are two main criteria, (1) when kinetic energy of deformation materials do not exceed approximately 5–10% of internal energy during the mostly simulation time, the adoptive mass scaling factor is reasonable, and (2) in order to obtain smooth solutions, it is

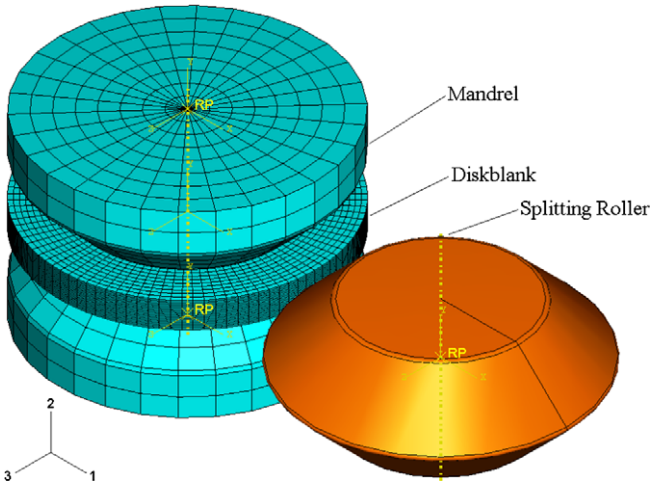

Fig. 4. FE model of hot splitting spinning under the ABAQUS/Explicit (for meshing).

necessary to validate whether the curve of kinetic energy is adequately smooth [32].

The relative values between Kinetic energy (ALLKE) and Internal energy (ALLIE) for whole model is shown in Fig. 5. According to Fig. 5, at the steady forming stage, the relative values between Kinetic energy and Internal energy is less than 5% obviously, so the curve satisfies the first criterion. The variations of Kinetic energy for whole model is shown in Fig. 6. According to Fig. 6, the Kinetic energy reaches a peak value in a short time, and then keeps steady state all the time, so the curve satisfies the second criterion. Therefore, this 3D elastic–plastic coupled thermo-mechanical FE model of hot splitting spinning of magnesium alloy AZ31 is reliable, steady and usable.

3. Results and discussion

Based on the above established reliable, steady and usable FE model, this study adopts the temperature-dependent thermal conductivity, thermal expansion coefficient, Young's modulus and specific heat for magnesium alloy AZ31 (density: 1780 kg/m^3, Poisson ratio: 0.33) listed in Tables 1–4 [8,33] and processing parameters of hot splitting spinning listed in Table 5 to numerical simulate. The field distributions of deformed component, including temperature fields, stress fields and strain fields, and the variation of different nodal temperature are obtained, and the influencing laws of different initial temperatures of disk blank and different feed rates of splitting roller on the quality and precision of deformed flanges are investigated, consequently the optimal forming temperature and the optimal feed rate of splitting roller during the hot splitting spinning process of magnesium alloy AZ31 are determined.

3.1. Temperature fields

During the hot splitting spinning process of magnesium alloy AZ31, because of the heat exchange between Diskblank and the external environment or the heat loss and the uneven interior heat source caused by the inhomogeneous deformation of Diskblank, the inner temperature gradient of deformed Diskblank are very large [34,35]. Temperature field distributions of Diskblank during the process is shown in Fig. 7. According to Fig. 7, temperature field distributions of Diskblank are very uneven, and the temperature of deformed section of Diskblank is much higher than that of undeformed section. The temperature of inner section of Diskblank contacting with roller is higher than that of bilaterally symmetrical sections of Diskblank contacting with mandrels. The former temperature reaches about 270 °C and the latter temperature is just about 220 °C, as shown in Fig. 7a, and the former temperature

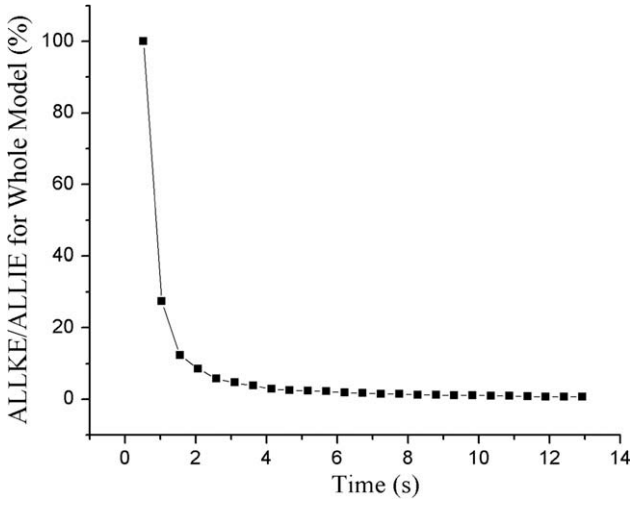

Fig. 5. The relative values between kinetic energy and internal energy for whole model.

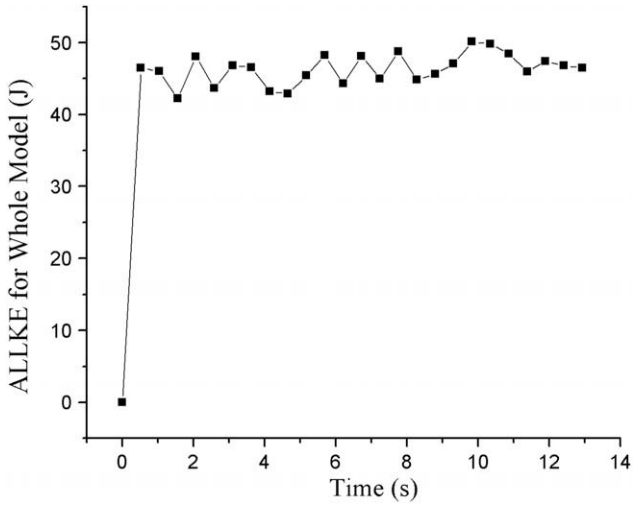

Fig. 6. The variations of kinetic energy for whole model.

Table 1
Thermal conductivity of magnesium alloy AZ31.

Temperature, °C	Thermal conductivity, W/(m °C)
96.4	25
101	100
105	200
109	300
113	400

Table 2
Thermal expansion coefficient of magnesium alloy AZ31.

Temperature, °C	Expansion coefficient, °C^{-1}
100	2.64E−005
200	2.7E−005
300	2.79E−005

Table 3
Young's modulus of magnesium alloy AZ31.

Temperature, °C	Young's modulus, GPa
20	40.2
75	37.3
100	34.3
125	30.9
150	30.4
200	29.4
250	27.5

Table 4
Specific heat of magnesium alloy AZ31.

Temperature, °C	Specific heat, J/(kg °C)
20	1050
100	1130
200	1170
300	1210
350	1260

Table 5
Processing parameters of hot splitting spinning.

Initial diameter of Diskblank, mm	100.0
Initial thickness of Diskblank, mm	10.0
Diameter of SplittingRoller, mm	99.17
Splitting angle of SplittingRoller, degree	45.0
Radius of corner of SplittingRoller, mm	1.0
Feed rate of SplittingRoller, mm/s	1.0
Rotational speed of Mandrels, rpm	98.0
Dimension of Mandrels, mm	100.0
Friction coefficient between Diskblank and SplittingRoller	0.15
Friction coefficient between Diskblank and Mandrels	0.15
Temperature of environment, °C	20
Temperature of dies, °C	200
Initial temperature of Diskblank, °C	300
Heat transfer coefficient (Diskblank-dies), W/(m^2 °C)	2000
Heat transfer coefficient (Diskblank-environment), W/(m^2 °C)	20

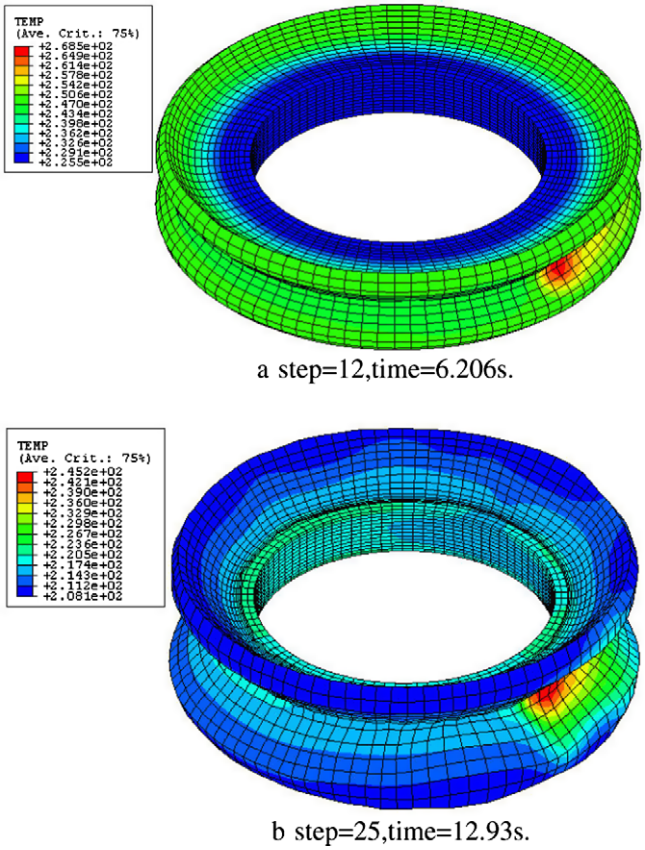

Fig. 7. Temperature field distributions of Diskblank.

reaches about 250 °C and the latter temperature is just about 210 °C, as shown in Fig. 7b. It is because friction and plastic deformation produce heat during the process, but the type of contact is surface contact and the temperature difference between dies and Diskblank is relatively large, so as to appear the large temperature gradients.

3.2. Nodal temperatures

In order to study the variations of different nodal temperatures for the whole disk blank, the location of trace points, including point A, point B and point C in the middle layer of disk blank and point D, point E and point F in the upper layer of disk blank, are shown in Fig. 8. The variations of temperatures with time at different trace points during the process are shown in Fig. 9. According

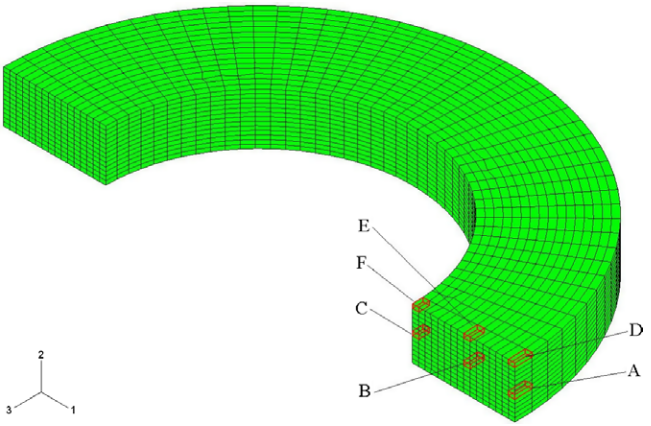

Fig. 8. Location of trace points.

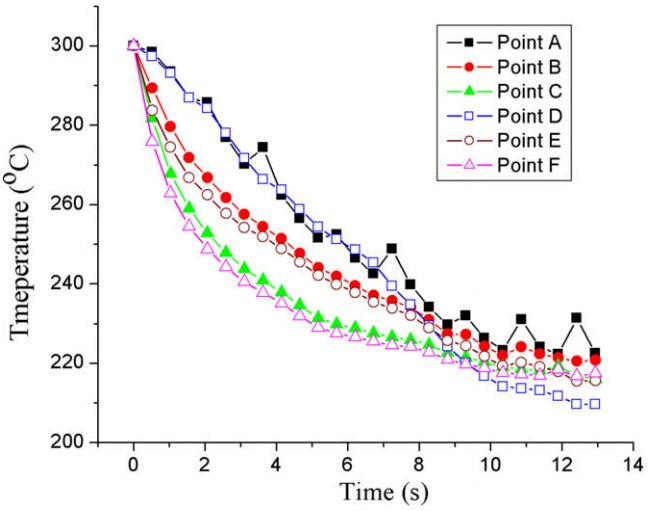

Fig. 9. Variations of temperatures with time at different trace points.

to Fig. 9, the temperature variations between point A and point D is similar, so do point B and point E as well as point C and point F. Point A and point D are both the trace points of outer circumferential surface of disk blank, but point A contacting with roller in the middle layer belongs to local plastic deformation zone and point D contacting with mandrels in the upper layer belongs to deformed flanges zone. Although the curves between point A and point D is similar, the temperature of point A reaches one extremum at intervals at the ending stage of the process and the extremum is a little more than that of point D. Because at the ending stage of the process, the deformation heat leads to ascend at intervals at point A after the temperature of point A goes down to about 240 °C. Besides, point A obtains the contact heat, radiation and friction heat, so that the temperature of point A is more than that of point D. Because of higher temperature of Diskblank, heat exchange exists between dies and environment. There is no enough time to exchange heat with the outside at the beginning of simulation, but as the simulation going on, external temperature of Diskblank descends, so there is a temperature gradient between inside and outside of Diskblank leading to the heat is transferred to the outside of Diskblank.

The curve of point B is extremely similar to the curve of point E and the curve of point C is also extremely similar to the curve of point F, but the temperature of point B is a little more than that

of point E and the temperature of point C is a little more than that of point F. The point in the middle layer of disk blank lies on the local plastic deformation zone, so more deformation heat is obtained. For the temperature distributions in the same layer of disk blank, the temperature of point A is more than that of point B and the temperature of point B is more than that of point C, and meanwhile the temperature of point D is more than that of point E and the temperature of point E is more than that of point F. The reasons are that, the deformation of outside circumferential zone is larger, and meanwhile the deformation energy and friction heat is larger than heat transferred from the surface to the environment. So, the temperature of point A and that of point D are relatively higher.

3.3. Strain fields

The logarithmic strain vector distributions at the ending stage of deformation are shown in Fig. 10. The logarithmic strain can reflect the accumulative effects of plastic deformation and metal flow directions. Therefore, the upper surface of deformed flanges contacting with mandrels and the under surface of deformed flanges contacting with roller both perform the tensile stress during the hot splitting spinning process of magnesium alloy AZ31, including section A and section C, as shown in Fig. 10. This state leads to the increase of deformed flanges steadily. But Diskblank in section A and section C will fracture on condition that larger tensile stress. The middle part of deformed flanges performs the compressive stress during the process, including section B, as shown in Fig. 10. This state leads to deformed flanges being more regular figures and higher quality and precision. But Diskblank in section B will wrinkle on condition that larger compressive stress.

The variations of equivalent plastic strain fields with time during the hot splitting spinning process of magnesium alloy AZ31 are shown in Fig. 11. Compared with the past research on cold splitting spinning [21], the temperature of two flanges is higher than that of local plastic deformation zone of flanges during the process due to deformed flanges contacting with both roller and mandrels. Consequently, there are two symmetrical belts in which equivalent strain distributions are uniform and even, as shown in Fig. 11b. Furthermore, due to the thermal plastic deformation, the maximum equivalent plastic strain of hot splitting spinning is more than the maximum equivalent plastic strain of cold splitting spinning.

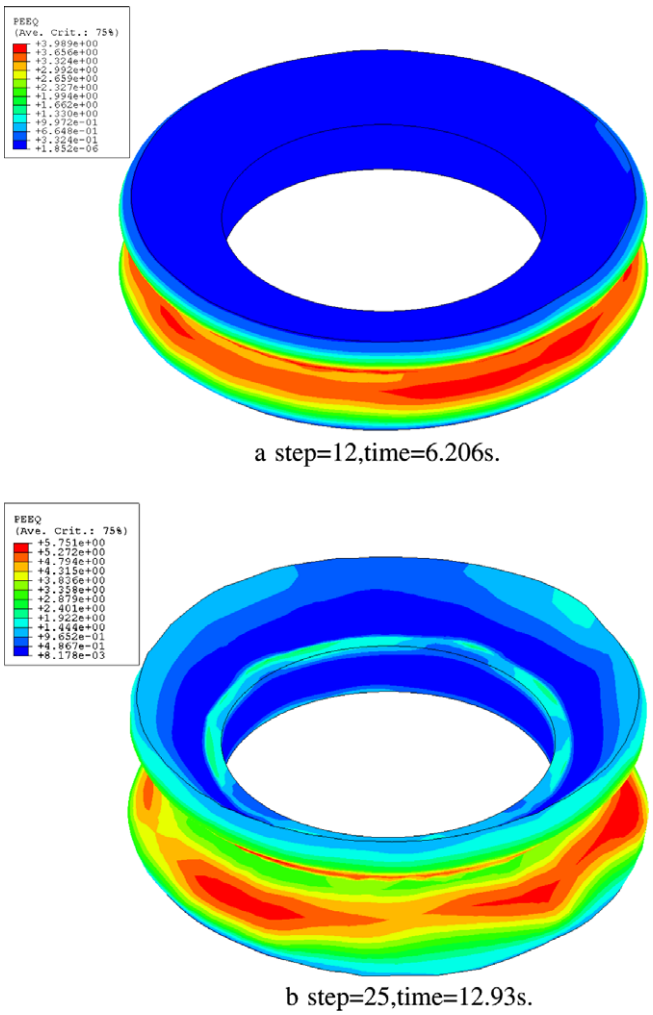

Fig. 11. The variations of equivalent plastic strain fields with time.

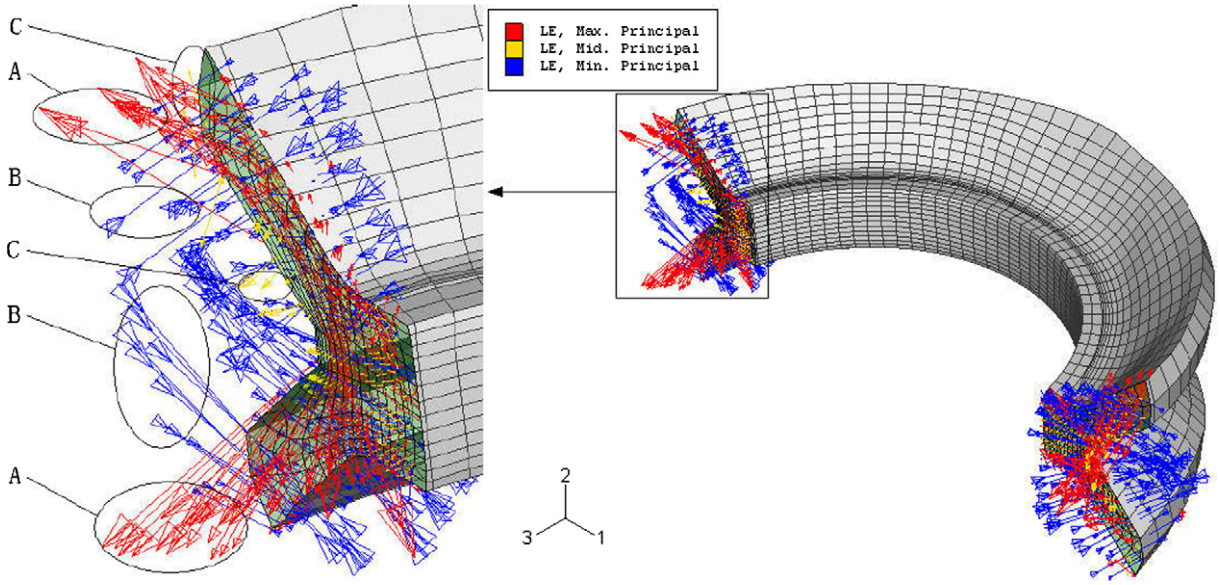

Fig. 10. Logarithmic strain vector distributions at the ending stage of deformation: A – red, B – blue, C – yellow. (For interpretation of the references to colour in this figure legend, the reader is referred to the web version of this article.)

3.4. Stress fields

The variations of equivalent stress fields with time during the hot splitting spinning process of magnesium alloy AZ31 are shown in Fig. 12. According to Fig. 12, compared with the past research on cold splitting spinning [21], stress concentration are not presented in the local plastic deformation zone contacting with roller due to the existence of softening process from DRX. There are enough heat for DRX in the upper surface of disk blank, therefore stress concentration are presented in the zone contacting with mandrels. Furthermore, the figure of stress concentration zone is not like a belt, only a corresponding section contacting with local plastic deformation zone.

3.5. Forming quality of deformed flanges

Due to the existence of softening process from DRX, different initial temperatures of disk blank and different feed rates of splitting roller have the important effects on the forming quality and precision of deformed flanges, so the corresponding influencing laws must be investigated. To study the influencing laws of different initial temperatures of disk blank and different feed rates of splitting roller on the forming quality and precision of deformed flanges, the quantitative evaluations of deformed flanges are as following [22], including thickness deviation of flanges $-\delta_t$ and angle deviation of inner-face/outer-face $-\delta_1/\delta_2$. The definition of the responding geometries of the roller and the disk blank is shown in Fig. 13. The thickness deviation of flanges $-\delta_t$ is expressed by

$$\delta_t = \frac{t - t_0}{t_0} \times 100\%, \tag{2}$$

where t is the thickness of simulation results and t_0 is the standard thickness. The angle deviation of inner-face $-\delta_1$, which contacts with the surfaces of roller, is expressed by

$$\delta_1 = \frac{\alpha_1 - \alpha_0}{\alpha_0} \times 100\%, \tag{3}$$

where α_1 is the angle of inner-face of flanges and α_0 is the standard angle. The angle deviation of outer-face $-\delta_2$, which contacts with the surfaces of mandrels, is expressed by

$$\delta_2 = \frac{\alpha_2 - \alpha_0}{\alpha_0} \times 100\%, \tag{4}$$

where α_2 is the angle of outer-face of flanges and α_0 is the standard angle.

The influencing laws of initial temperature of Diskblank on thickness deviation of deformed flanges are shown in Fig. 14. According to Fig. 14, in the defined scope of initial temperature of Diskblank, thickness deviation of deformed flanges decreases distinctly at the beginning stage, and then is close to approximately zero when temperature is 300 °C, and increases gradually with the increase of forming temperature, and finally reaches about 2%.

The influencing laws of initial temperature of Diskblank on angle deviation of deformed flanges are shown in Fig. 15. According to Fig. 15, in the defined scope of initial temperature of Diskblank, the angle deviation of outer-face is a little more than that of inner-face, and they remain with the similar curves. The curves decreases distinctly at the beginning stage, and then increases gradually with the increase of forming temperature. When temperature is 300 °C, both angle deviations of deformed flanges are close to approximately zero simultaneously.

The influencing laws of feed rate of splitting roller on thickness deviation of deformed flanges are shown in Fig. 16. According to Fig. 16, in the defined scope of feed rate of splitting roller, there are three phases for the changing curve. When $v < 1$ mm/s, thickness deviation of deformed flanges increases distinctly and are negative. When $1 \leqslant v \leqslant 3$ mm/s, thickness deviation holds approximately zero. When $v > 3$ mm/s, thickness deviation increases gradually and are positive, and the value is more than 4%.

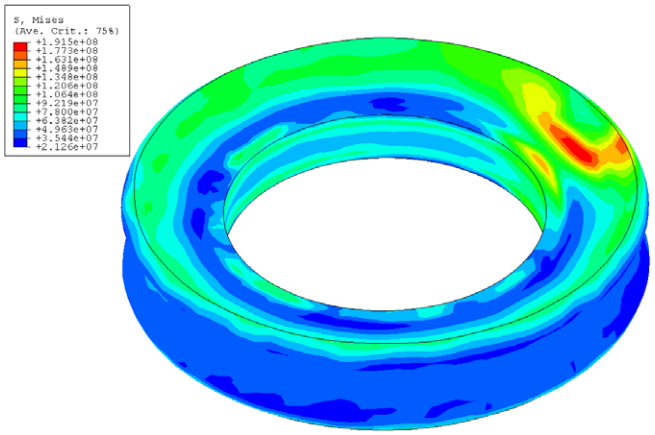

a step=12,time=6.206s.

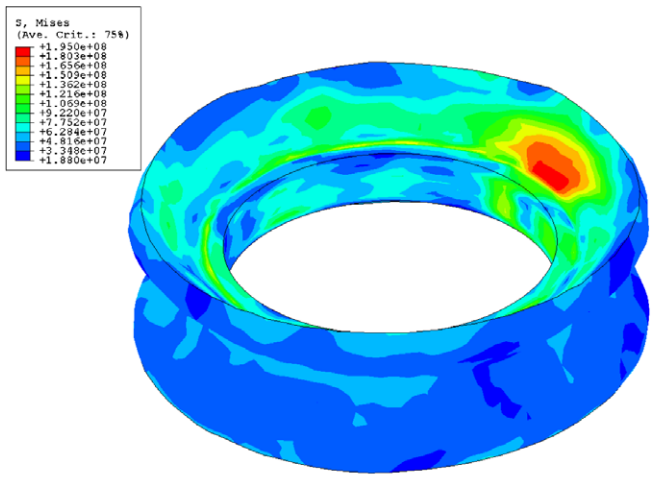

b step=25,time=12.93s.

Fig. 12. The variations of equivalent stress fields with time.

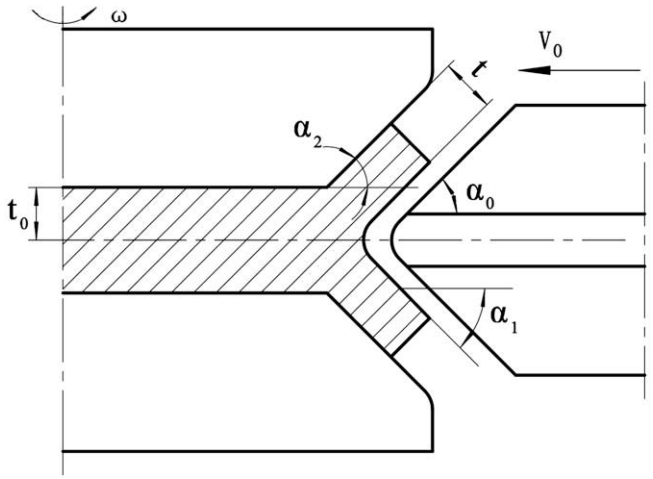

Fig. 13. The definition of the responding geometries of the roller and the disk blank.

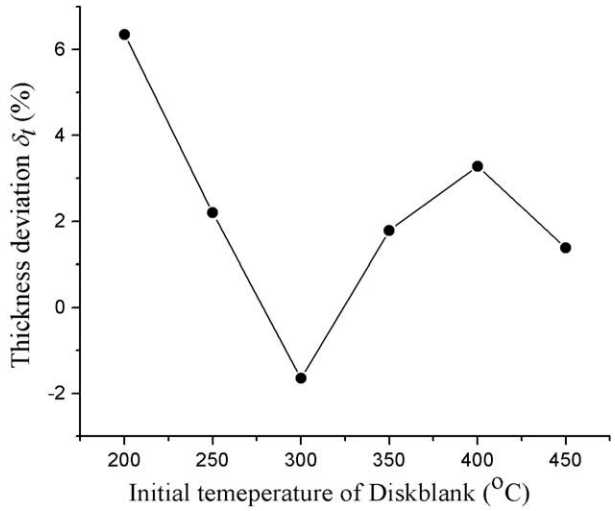

Fig. 14. The influencing laws of initial temperature of Diskblank on thickness deviation.

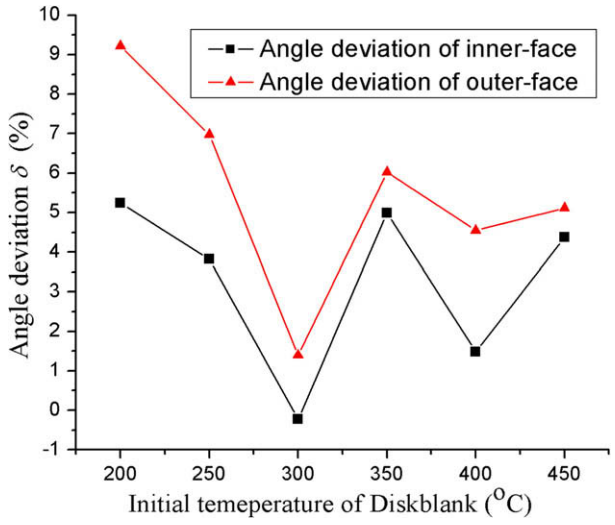

Fig. 15. The influencing laws of initial temperature of Diskblank on angle deviation.

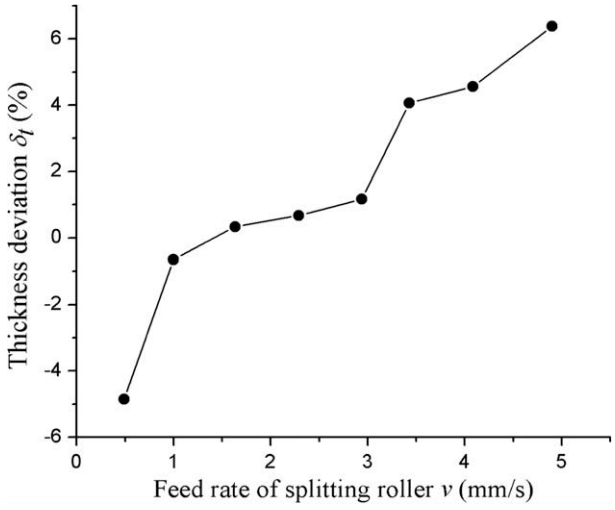

Fig. 16. The influencing laws of feed rate of splitting roller on thickness deviation.

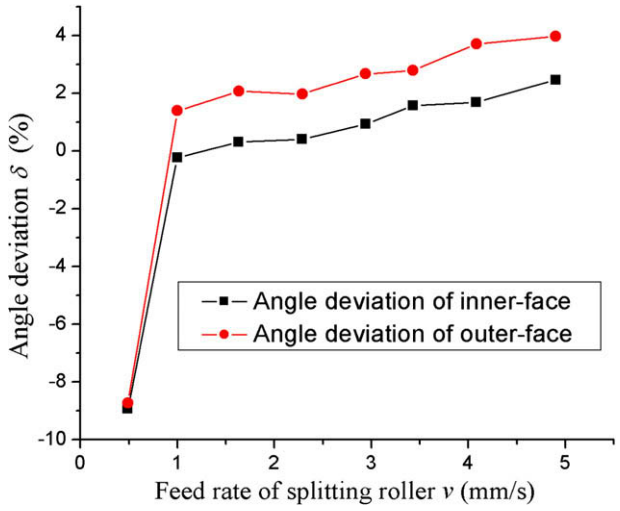

Fig. 17. The influencing laws of feed rate of splitting roller on angle deviation.

The influencing laws of feed rate of splitting roller on angle deviation of deformed flanges are shown in Fig. 17. According to Fig. 17, in the defined scope of feed rate of splitting roller, when $v < 1$ mm/s, angle deviation of deformed flanges increases suddenly and are negative, and the values are less than −8%; when $1 \leqslant v \leqslant 3$ mm/s, angle deviation hold approximately from 0% to 2%; when $v > 3$ mm/s, angle deviation increases gradually, and angle deviation of inner-face reaches above 2% and angle deviation of outer-face reaches above 4%.

The above two quantitative evaluations of deformed flanges are relatively larger values when temperature is about 200 °C, namely, for initial temperature of Diskblank, thickness deviation is more than 6%, angle deviation of inner-face is more than 9% and angle deviation of outer-face is more 5%, and meanwhile for feed rate of splitting roller, thickness deviation is less than −5%, angle deviation of inner-face and outer-face are both less than −9%. And when temperature is about 450 °C, the above two quantitative evaluations of deformed flanges become even and steady, but larger values, namely, for initial temperature of Diskblank, thickness deviation is more than 4%, angle deviation of inner-face is more than 6% and angle deviation of outer-face is more 5%, and meanwhile for feed rate of splitting roller, thickness deviation is more than 6%, angle deviation of inner-face and outer-face are both less than 4%. Only when forming temperature is about 300 °C, the above two quantitative evaluations of deformed flanges are close to zero. The reasons are that, strain hardening and softening from DRX keep an appropriate balance during the hot splitting spinning process of magnesium alloy AZ31 when temperature is about 300 °C, so here thickness deviation is minor and angle deviation is close to zero, and forming quality and precision are highest. In the same way, when the feed rate of splitting roller is defined from 1 to 3 mm/s, forming quality and precision are also highest during the hot splitting spinning process of magnesium alloy AZ31. Consequently, the optimal forming temperature is approximate 300 °C and the optimal feed rate of splitting roller ranges from 1 to 3 mm/s during the hot splitting spinning process of magnesium alloy AZ31.

4. Conclusions

In this study, based on the coupled thermo-mechanical simulation of the hot splitting spinning process of magnesium alloy AZ31, the forming characteristics and laws during the process are as follows:

(1) During the process, temperature field distributions of Diskblank are very uneven, and the temperature of inner section of Diskblank contacting with roller is higher than that of bilaterally symmetrical sections of Diskblank contacting with mandrels, so there is a temperature gradient between inside and outside of Diskblank.
(2) During the process, section A and section C (Fig. 10) perform the tensile stress, and this state leads to the increase of deformed flanges steadily; section B (Fig. 10) performs the compressive stress, and this state leads to deformed flanges being more regular figures and higher quality and precision. There are two symmetrical uniform belts in the equivalent strain distributions, and the stress concentration are presented in only one section contacting with mandrels.
(3) The optimal forming temperature is approximate 300 °C and the optimal feed rate of splitting roller ranges from 1 to 3 mm/s during the hot splitting spinning process of magnesium alloy AZ31.

Acknowledgements

The authors would like to thank the National Natural Science Foundation of China (Nos. 50405039 and 50575186), the National Science Found of China for Distinguished Young Scholars (No. 50225518), the National "863" Project of China (No. 2008AA04Z122) and the Foundation of NWPU (No. W018104) for the support given to this research.

References

[1] M. Michael, Avedesian, Hugh Baker, Magnesium and Magnesium Alloys, ASM Specialty Handbook, 1999.
[2] B.L. Mordike, T. Ebert, Mater. Sci. Eng. A 302 (2001) 37–45.
[3] Sabbah Ataya, Essam El-Magd, Comput. Mater. Sci. 39 (2007) 155–159.
[4] C.C. Wong, T.A. Dean, J. Lin, Int. J. Mach. Tools Manuf. 43 (2003) 1419–1435.
[5] Wang Chenghe, Liu Kezhang, Spinning Technology, China Machine Press, Beijing, 1986 (in Chinese).
[6] H. Yang, M. Zhan, Y.L. Liu, F.J. Xian, Z.C. Sun, Y. Lin, X.G. Zhang, J. Mater. Process. Technol. 151 (2004) 63–69.
[7] N. Bontcheva, G. Petzov, Comput. Mater. Sci. 34 (2005) 377–388.
[8] R.J. Gu, H. Yang, M. Zhan, H. Li, H.W. Li, Comput. Mater. Sci. 42 (2008) 537–549.
[9] Y.H. Song, K.F. Zhang, Z.R. Wang, F.X. Diao, J. Mater. Process. Technol. 97 (2000) 35–43.
[10] Qun-Feng Chang, Da-Yong Li, Ying-Hong Peng, Xiao-Qin Zeng, Int. J. Mach. Tools Manuf. 47 (2007) 436–443.
[11] G. Palumbo, D. Sorgente, L. Tricarico, S.H. Zhang, W.T. Zheng, J. Mater. Process. Technol. 191 (2007) 342–346.
[12] N. Ogawa, M. Shiomi, K. Osakada, Int. J. Mach. Tools Manuf. 42 (2002) 607–614.
[13] E. Doege, K. Droder, J. Mater. Process. Technol. 115 (2001) 14–19.
[14] Chen Zhenhua, Deformation Magnesium Alloys, Chemical Industry Press, Beijing, 2005 (in Chinese).
[15] Jaroslav Mackerle, Comput. Mater. Sci. 31 (2004) 187–219.
[16] Jaroslav Mackerle, Comput. Mater. Sci. 27 (2003) 313–332.
[17] H. Grass, C. Krempaszky, T. Reip, E. Werner, Comput. Mater. Sci. 28 (2003) 469–477.
[18] H. Grass, C. Krempaszky, E. Werner, Comput. Mater. Sci. 36 (2006) 480–489.
[19] Stefan Hauk, Victor H. Vazquez, Taylan Altan, J. Mater. Process. Technol. 98 (2000) 70–80.
[20] Dieter Schmoeckel, Stefan Hauk, J. Mater. Process. Technol. 98 (2000) 65–69.
[21] Liang Huang, He Yang, Mei Zhan, Comput. Mater. Sci. 42 (2008) 643–652.
[22] Liang Huang, He Yang, Mei Zhan, Lijin Hu, Comput. Mater. Sci. 45 (2009) 449–461.
[23] Huang Liang, Yang He, Zhan Mei, Hu Li-jin, Trans. Nonferr. Met. Soc. China 18 (2008) 674–681.
[24] Liang Huang, He Yang, Mei Zhan, Yuli Liu, J. Mater. Process. Technol. 201 (2008) 267–272.
[25] A. Staroselsky, L. Anand, Int. J. Plast. 19 (2003) 1843–1864.
[26] Yasumasa Chino, Katsuya Kimura, Masataka Hakamada, Mamoru Mabuchi, Mater. Sci. Eng. A 485 (2008) 311–317.
[27] Yasumasa Chino, Katsuya Kimura, Mamoru Mabuchi, Mater. Sci. Eng. A 486 (2008) 481–488.
[28] Juan Liu, Zhenshan Cui, Congxing Li, Comput. Mater. Sci. 41 (2008) 375–382.
[29] Yu Hanqing, Chen Jinde, The Principle of Metal Plastic Forming, China Machine Press, Beijing, 1999 (in Chinese).
[30] Getting Started with ABAQUS (Version 6.4), ABAQUS Inc., 2004.
[31] ABAQUS Analysis User's Manual (Version 6.4), ABAQUS Inc., 2004.
[32] M. Hayama, T. Murota, Kudo Hi, Bull. JSME 31 (1965) 453–460.
[33] Zhang Jin, Zhang Zonghe, Magnesium Alloy and Its Application, Chemical Industry Press, Beijing, 2004 (in Chinese).
[34] C. Messner, E.A. Werner, Comput. Mater. Sci. 26 (2003) 95–101.
[35] C.S. Wu, J.S. Sun, Comput. Mater. Sci. 25 (2002) 457–468.